

1 From Canals to the Coast: Dissolved Organic Matter and Trace 2 Metal Composition in Rivers Draining Degraded Tropical 3 Peatlands in Indonesia

4 Laure Gandois^a, Alison M. Hoyt^{b*}, Stéphane Mounier^c, Gaël Le Roux^a, Charles F. Harvey^{bd},
5 Adrien Claustres^a, Mohammed Nuriman^e, Gusti Anshari^c

6 ^a EcoLab, Université de Toulouse, CNRS, INPT, UPS, Toulouse, France

7 ^bDepartment of Civil & Environmental Engineering, Massachusetts Institute of Technology, Cambridge, MA
8 01239, USA

9 ^cPROTEE, Université de Toulon, F-83957, La Garde, France

10 ^d Center for Environmental Sensing and Modeling, Singapore MIT Alliance for Research and Technology,
11 Singapore

12 ^eMagister of Environmental Science, and Soil Science Department, Universitas Tanjungpura (UNTAN),
13 Pontianak, West Kalimantan Province, Indonesia

14 *Present address: Max Planck Institute for Biogeochemistry, 07745 Jena, Germany

15 Corresponding author: ahoyt@bgc-jena.mpg.de
16

17 **Abstract.** Worldwide, peatlands are important sources of dissolved organic matter (DOM) and trace metals (TM)
18 to surface waters and these fluxes may increase with peatland degradation. In Southeast Asia, tropical peatlands
19 are being rapidly deforested and drained. The black rivers draining these peatland areas have high concentrations
20 of DOM, and the potential to be hotspots for CO₂ release. However, the fate of this fluvial carbon export is
21 uncertain, and its role as a trace metal carrier has never been investigated. This work aims to address these gaps in
22 our understanding of tropical peatland DOM and associated elements in the context of degraded tropical peatlands
23 in Indonesian Borneo. We quantified dissolved organic carbon and trace metal concentrations in the dissolved and
24 fine colloidal (<0.22µm) and coarse colloidal (0.22 – 2.7 µm) fractions and determined the characteristics ($\delta^{13}\text{C}$,
25 Absorbance, Fluorescence: excitation-emission matrix and PARAFAC analysis) of the peatland-derived DOM as
26 it drains from peatland canals, flows along the Ambawang River (black river), and eventually mixes with the
27 Kapuas Kecil River (white river) before meeting the ocean near the city of Pontianak in West Kalimantan,
28 Indonesia. We observe downstream shifts in indicators of in-stream processing. An increase in the $\delta^{13}\text{C}$ of DOC,
29 along with an increase in the C1/C2 ratio of PARAFAC fluorophores, and decrease in SUVA (Specific UV
30 Absorbance) along the continuum suggest the predominance of photo-oxidation. However, very low dissolved
31 oxygen concentrations also suggest that oxygen is quickly consumed by microbial degradation of DOM in the
32 shallow layers of water. Black rivers draining degraded peatlands show significantly higher concentrations of Al,
33 Fe, Pb, As, Ni, and Cd, compared to the white river. A strong association is observed between DOM, Fe, As, Cd
34 and Zn in the dissolved and fine colloid fraction, while Al is associated with Pb and Ni and present in a higher
35 proportion in the coarse colloidal fraction. We additionally measured the isotopic composition of lead released
36 from degraded tropical peatlands for the first time and show that Pb originates from anthropogenic atmospheric

37 deposition. Degraded tropical peatlands are important sources of DOM and trace metals to rivers and a secondary
38 source of atmospherically deposited contaminants.

39 **Keywords:** Tropical peatlands, Dissolved Organic Matter, Absorbance, Fluorescence, PARAFAC, Stable
40 isotopes, Trace metal, Lead isotopes

41 **1. Introduction**

42 Most Southeast Asian tropical peatlands developed as domes beneath ombrotrophic peat swamp forests (Page et
43 al., 2006; Cobb et al. 2017). They store at least 68.5 Pg C, or 15-19% of the global peat carbon stocks (Dargie et
44 al., 2017; Lahteenoja et al., 2009; Page et al., 2011). They have experienced widespread degradation as a result of
45 deforestation, conversion to agriculture and drainage, which all accelerated in the late 2000s. This abrupt change
46 in land use, and corresponding lowering of the water table, has led to subsidence and a massive release of carbon
47 from peatlands to the atmosphere due to enhanced aerobic decomposition of organic matter from the drained peat.
48 Extensive work has focused on quantifying the resulting CO₂ fluxes (Couwenberg et al., 2010; Hoyt et al., 2019;
49 Jauhiainen et al., 2012; Miettinen et al., 2017) and land surface subsidence (e.g. Hooijer et al., 2012; Carlson et
50 al., 2015).

51 Drainage canals are dug in forested peatlands for multiple reasons: first, as a mechanism to transport timber out of
52 the peatland during deforestation, and later to lower the water table, making the land suitable for agriculture. These
53 peatland drainage canals channel water from the peatlands to surrounding surface waters. The resulting fluvial
54 export of dissolved organic matter (DOM) has been recognized as an important component of the carbon budget
55 of tropical peatlands, that could increase with deforestation and peatland exploitation (Gandois et al., 2013; Moore
56 et al., 2011). Indonesia alone contributes over 10% of the global riverine dissolved organic carbon (DOC) input
57 into the ocean (Baum et al., 2007), as a result of both high peatland coverage and high precipitation rates. This
58 proportion is likely to increase with rapid peatland conversion to agriculture, which destabilizes long-term peat C
59 stocks (Moore et al., 2013).

60 Another implication of DOM transfers from peatlands to surface water is the transport of associated elements,
61 especially trace metals (TM). Tropical peatlands in Southeast Asia are mainly ombrotrophic systems, which
62 receive critical nutrients through atmospheric deposition, and serve as a sink for atmospheric pollutants (Weiss et
63 al., 2002). Northern peatlands have been shown to constitute a source of major and trace elements to surface waters
64 (Broder and Biester, 2017; Jeremiason et al., 2018; Rothwell et al., 2007). This has important implications: as a
65 result of colloidal association between peatland-derived organic molecules and Fe, northern peatlands are
66 responsible for a significant transfer of Fe to the Atlantic Ocean (Krachler et al. 2010, 2012). In the UK, peat
67 degradation and erosion has led to the dispersion of lead into watersheds, which previously accumulated through
68 atmospheric deposition over decades (Rothwell et al., 2008). Although drainage of tropical peatlands is occurring
69 at a rapid rate across Southeast Asia, to our knowledge no data are available on trace metal release in black rivers
70 draining tropical peatlands.

71 Black rivers draining peatlands (as defined in Alkhatib et al., (2007)) also have the potential to be hotspots of
72 fluvial carbon degassing (Muller et al., 2015; Wit et al., 2015). By measuring pCO₂ in Indonesian and Malaysian

73 black rivers, Wit et al. (2015) estimated that 53% of DOC entering surface waters was converted to CO₂, which is
74 similar to global averages for inland waters. In contrast, black river measurements and incubations by Martin et
75 al., (2018) found a smaller proportion of DOC was processed in rivers. Rixen et al., (2008) also found a large
76 proportion of the DOM was resistant to decomposition in a laboratory incubation study. These studies have focused
77 on CO₂ measurements and incubations to assess the potential for DOM processing.

78 Monitoring both isotopic and optical characteristics of DOM composition in canals and rivers can provide
79 complementary information on the extent of in-stream processing of fluvial carbon, and potential emission of
80 greenhouse gases (GHGs) to the atmosphere. Qualitative evaluation of in-stream DOM transformation by UV light
81 and microbial processes can be performed using isotopic and optical characterization of DOM. The stable isotope
82 signature of DOM is both an indicator of its origin (Barber et al., 2017; Hood et al., 2005), as well as transformation
83 processes. Lalonde et al. (2014) assessed photochemical processing of DOM in major rivers worldwide, and found
84 that it caused an increase in the $\delta^{13}\text{C}$ of DOM of 0.5 to 2.3‰. Similarly, microbial processing is also expected to
85 lead to an increase in the $\delta^{13}\text{C}$ of DOM. Optical properties of DOM are also sensitive indicators of DOM processing
86 (Hansen et al., 2016; Harun et al., 2015; Spencer et al., 2009). However, in contrast to the $\delta^{13}\text{C}$ of DOM, which is
87 similarly enriched by both microbial processing and photo-oxidation, the optical properties of DOM change in
88 opposite directions in response to microbial processing or photo-oxidation. Microbial processing is generally found
89 to increase the aromaticity of DOM by selective processing of less aromatic molecules, while photo-oxidation
90 tends to decrease aromaticity, because of selective photo-oxidation of aromatic moieties (Spencer et al., 2009;
91 Hansen et al., 2016).

92 In summary, although there has been an increase in efforts to quantify DOC exports from tropical peatlands, our
93 complementary understanding of the transfer of associated elements and in-stream processing of DOM remains
94 limited. This work aims to address these gaps in our understanding of the composition and evolution of tropical
95 peatland DOM and how it could act as a carrier of trace metals to surface waters, in the context of highly degraded
96 tropical peatlands in Indonesia. We characterize the quality of the peatland-derived DOM and trace metals as they
97 drain from peatland canals, flow along black rivers, and eventually mix with a white water river before meeting
98 the ocean. We assess spatial and seasonal changes in the organic matter quality, and document changes in DOM
99 composition due to transport, mixing, and processing. We also assess black river trace metal release to surface
100 waters, analyzing trace metal concentrations and the isotopic composition of lead released from degraded tropical
101 peatlands for the first time.

102 **2. Material and methods**

103 **2.1 Study area**

104 The study area is located in West Kalimantan, Indonesia, near the city of Pontianak (0.09°N, 109.24°E) on the
105 island of Borneo (Figure 1). The climate is humid equatorial with 2953±564 mm of rainfall and a mean annual
106 temperature of 27°C (1985-2017 data). The average monthly rainfall ranges from 170±126 mm (August) to 349±98
107 mm (November). The highest rainfalls are measured from October to January. The mean rainfall is 274 ± 123 mm
108 for January, and 199 ± 106 mm for June. (Figure SI.1). The study focused on the Ambawang River, which flows
109 into the Landak river, which in turn flows into Kapuas Kecil river. It is a black river draining a watershed

110 (approximately 706 km²) entirely covered with peatlands. This river was selected to represent water of
111 exclusively peatland origin. All peatlands in the sampling area have been drained and converted to agriculture.
112 Current land use consists of small scale rubber plantation, secondary forest, oil palm plantation, and human
113 settlements.

114 **2.2 Sample collection and treatment**

115 Two sampling campaigns were conducted in June 2013 (drier period) and January 2014 (wetter period). Using a
116 boat, samples were collected in the center of the river, from the origin of the Ambawang river (BR, black river
117 sites) to its downstream confluence with the Landak and Kapuas Kecil Kecil (WR, white river sites). White river
118 samples collected upstream of the confluence with the white river (WRu, white river upstream). Drainage canals
119 (DC) flowing into the black river were also sampled during the second sampling campaign (Figure 1). In January
120 2014, a rain collector was installed on the roof of the Pontianak's meteorological station to collect rain samples
121 for lead isotopic analysis. In situ parameters (pH, conductivity and dissolved oxygen) were measured using a
122 multiparameter probe (WTW, Germany). Depth profiles of dissolved oxygen in the black river were also measured
123 with an oxygen microelectrode (MI-730 dip-type micro-oxygen electrode and O2-ADPT adapter; Microelectrodes,
124 Inc., Bedford, NH, USA). Frequent calibration was performed with a zero oxygen solution and distilled water
125 equilibrated to ambient oxygen concentrations, where temperature was carefully monitored. To create the zero
126 oxygen solution, 1 g of sodium sulfite (Na₂SO₃) and a few crystals (~1 mg) of cobalt chloride (CoCl₂) was
127 dissolved in 1 L of distilled water. For measurements of additional parameters, a larger volume of water was
128 collected for further analysis. Samples were filtered immediately following collection on the boat using a portable
129 peristaltic pump (Geotech, USA) and prebaked (5h, 450°C) and pre-weighed GF/F filters (0.7 µm) and stored in
130 glass bottles for DOC, δ¹³C-DOC and optical properties of DOM analysis, and acidified with HCl for DOC and
131 δ¹³C-DOC. Samples were filtered with cellulose acetate filters (0.22 µm), acidified with HNO₃ and stored in
132 polypropylene vials for analysis of major nutrients and trace element. DOC analysis was repeated on the cellulose
133 acetate samples and DOC concentrations did not differ significantly based on filtration at 0.2 or 0.7 µm. In January
134 2014, at selected sites (8), samples were first filtered with GF/D filters (2.7µm) to assess to the coarse colloidal
135 fraction of trace metals and DOC.

136 **3. Sample analysis**

137 Non-purgeable organic carbon (NPOC, referred to hereafter as DOC) was analyzed on filtered (GF/F Whatman)
138 samples after acidification to pH 2 (HCl) with a TOC-V CSH analyzer (Shimadzu, Japan), with a quantification
139 limit of 1 mg L⁻¹. Major cations and anions were analysed using an HPLC (Dionex, USA). The quantification limit
140 was 0.5 mg L⁻¹ for chloride, nitrate and sulphates and 0.025 mg L⁻¹ for ammonium, potassium, magnesium and
141 calcium. Certified material (ion 915 and ion 96.4 Environment and Climate Change Canada, Canada) was included
142 in the analytical loop and recovery was >95% of the certified value. For trace element analysis, samples were
143 acidified with ultrapure HNO₃ prior to ICP-MS (7500 ce, Agilent Technologies) analysis. ¹¹⁵In was used as an
144 internal standard, and SLRS-4 (River water certified for trace elements) was used as a reference material on every
145 run and accuracy (recovery>95%) was checked. Determination limits were < 0.5 µg g⁻¹ for Fe and Al, <0.05 µg g⁻¹
146 ¹ for Ni, Cu and Zn and < 0.005 µg g⁻¹ for Cd and Pb. Pb isotope ratios (²⁰⁶Pb/²⁰⁷Pb; ²⁰⁸Pb/²⁰⁶Pb) in water samples

147 were analyzed using a High Resolution ICP-MS (Thermo Element II XR; OMP service ICP-MS, Toulouse,
148 France). Measurements were corrected for mass bias using individual sample bracketing with certified and
149 adequately diluted NIST NBS-981 (100 ng L⁻¹ to 500 ng L⁻¹) according to Krachler et al. (2004).

150 The UV absorption spectra of pore water were measured with a spectrophotometer (Secoman UVi-lightXT5) from
151 190 to 700 nm in a 1 cm quartz cell. The Specific UV Absorbance at 254 nm (SUVA, L mg⁻¹ m⁻¹) was calculated
152 as follows: $SUVA = A_{254}/(b \cdot DOC)$ (Weishaar et al., 2003), where A_{254} is the sample absorbance at 254 nm (non-
153 dimensional), b is the optical path length (m) and DOC is in mg L⁻¹. The baseline was determined with ultra-pure
154 water. Potential additional absorbance related to Fe content was examined following the procedure described by
155 Poulin et al., (2014). The additional absorbance was small, and represented only $3.6 \pm 1.4\%$ of the total absorbance
156 across all samples and was therefore neglected.

157 Emission Excitation Matrices (EEM) were acquired using a Hitachi F4500 fluorescence spectrometer, and
158 instrument specific correction were applied. Emission spectra were acquired from 250 to 550 nm for excitation
159 ranging from 250 to 550 nm. The slits were set to 5 nm for both the excitation and emission monochromators. The
160 scan speed was 2400 nm min⁻¹ and the integration response was 0.1 s. Fluorescence intensity was corrected from
161 the excitation beam to ensure stability. The inner filter effect water was taken into account using a dilution
162 approach as developed by Luciani et al. (2009). The fluorescence index was calculated as defined by McKnight et
163 al. (2001) and adapted by Jaffé et al. (2008), by the ratio of the fluorescence intensity at 470 nm to the fluorescence
164 intensity at 520 nm for a 370 nm excitation. The shape of the excitation spectra was checked following the
165 recommendation of Cory et al., (2010). The PARAFAC analysis (PARAllel FACtor analysis (Bro, 1997)) was
166 performed on all samples using the PROGMEEF program in Matlab (Luciani et al., 2008).

167 The isotopic composition ($\delta^{13}C$) of DOC was determined at the UC Davis Stable Isotope Facility, following the
168 described procedure (<http://stableisotopefacility.ucdavis.edu/doc.html>). Briefly, a TOC Analyzer (OI Analytical,
169 College Station, TX) is interfaced to a PDZ Europa 20-20 isotope ratio mass spectrometer (Sercon Ltd., Cheshire,
170 UK) utilizing a GD-100 Gas Trap Interface (Graden Instruments).

171 **4. Statistical analysis**

172 Statistical analysis was performed using R (R Core Team, 2019) and the R studio software (Version 1.2.1335),
173 using ggplot (Wickham, 2016), dplyr (Wickham et al., 2019), and dunn.test (Dinno, 2017) packages. Significant
174 differences ($p < 0.05$) between groups were evaluated using Kruskal Wallis and Dunn's post hoc multiple test.

175 **5. Results**

176 **5.1. Trends in water chemistry from the source of the black river to the ocean**

177 The observed water chemistry of the Ambawang river and drainage canals is typical of black rivers draining
178 peatlands (Table 1, Figure 2), and does not show significant differences between the two sampling seasons. It is
179 acidic with a pH of 3.2 ± 0.6 and 3.5 ± 0.3 in the drainage canals (DC) and black river (BR) respectively, has a
180 low conductivity (DC: $89.8 \pm 21.4 \mu S cm^{-1}$, BR: $85.2 \pm 21.6 \mu S cm^{-1}$), is hypoxic (DC: 2.3 ± 0.3 , BR: $1.9 \pm 0.7 mg$

181 L⁻¹), and has low nutrient concentrations (DIN < 0.3 mg L⁻¹ and P-PO₄ < 0.015 mg L⁻¹) but high DOC
182 concentrations (DC: 35.2 ± 5.9, BR: 35.8 ± 3.5 mg L⁻¹). The Cl⁻ concentrations are low and homogeneous (DC:
183 2.6 ± 0.7, BR: 2.4 ± 0.6 mg L⁻¹). After the confluence with the white river, the chemistry of the river radically
184 changes. An abrupt increase in pH is observed (WR: 5.3 ± 0.7). The dissolved oxygen concentration increases to
185 3.7±1.0 mg L⁻¹, while DOC concentrations drop sharply to 9.2 ± 3.2 mg L⁻¹. We also observe a slight increase in
186 NO₃⁻ and decrease in PO₄²⁻. Across all samples, the DOC concentrations show a significant negative correlation
187 with DO concentrations (r²=0.63, n=40, p<4.10⁹). In contrast, no increase in Cl⁻ concentration is observed until
188 close to the ocean (3 samples corresponding to ocean water intrusion were excluded from Figure 2).

189 **5.2. DOM optical characteristics and stable isotopic signature**

190 No systematic differences are observed for the DOM characteristics between the two sampling campaigns. The
191 δ¹³C signature of DOC (Figure 3a) is very negative, reaching -30.3±0.4‰ in the drainage canals. It gradually and
192 continually increases along the continuum from upstream in the black river to the ocean (Figure 3a). As a result,
193 the δ¹³C of DOC in the drainage canals and the black river, is significantly more depleted than the white river. The
194 δ¹³C signature of DOC is significantly negatively correlated with DOC concentration (r²=0.68, p<10⁻⁴, n=40), with
195 the highest DOC values being associated with the lowest δ¹³C-DOC values.

196 The SUVA index (Figure 3b) has high values in the black river (5.3±1.2), with the highest values measured
197 upstream. A wide range of values is measured in the drainage canals (4.3 ±1.4). The SUVA values of the black
198 river are significantly higher than those measured in the Kapuas Kecil (4.5±0.3) and its tributaries (4.2 ±0.2). The
199 fluorescence index has relatively high values for tropical peatlands, where most of the DOM originates is of
200 terrestrial origin (Gandois et al., 2014; Zhou et al., 2019). The FI values vary widely in the drainage canals
201 (1.60±0.17) and black river (1.55±0.06), but is more uniform in the white river, both upstream (1.55±0.03) and
202 downstream (1.55±0.05) of the confluence with the black river. Despite the high FI values, these two optical
203 indices show coherent spatial patterns within the black river and drainage canals (Figure 3b&d). For example,
204 lower SUVA values are associated with higher FI values, in three drainage canals and in the black river close to
205 their connection, sampled during the second sampling campaign. Across all samples, a significant correlation is
206 observed between FI and SUVA values (r²=0.37, p<10⁻⁴, n=41).

207 The EEMS of all water samples have two main peaks (Figure SI.2). The primary peak (λ_{ex}=250 nm, λ_{em}= 460
208 nm), is coupled with a less intense peak (λ_{ex}=350 nm, λ_{em}= 460 nm). The peaks are typical of high molecular
209 weight and aromatic molecules, which have been observed in wetlands (Fellman et al., 2009). The PARAFAC
210 analysis reveals two fluorophores: C1 (λ_{ex}=255 nm, λ_{em}= 450 nm) and C2 (λ_{ex}=285 nm, λ_{em}= 485 nm, Figure
211 SI. 3) The first component constitutes from 60 to 73 % of the total fluorescence of samples. The relative
212 contribution of these two fluorophores evolves along the sampled continuum, with the lowest values measured
213 upstream in the black river (Figure 3c). The spatial evolution of the C1/C2 ratios and the δ¹³C-DOC values show
214 consistent trends. A significant (r²=0.43, p< 0.001, n=41) relationship is observed across all the samples between
215 these two indicators. A stronger relationship (r²=0.85, p< 0.001, n=5) is observed when the drainage canals samples
216 alone are considered.

217 **5.3. Trace element concentrations and physical fractionation**

218 Black rivers originating from drained peatlands have a unique composition of inorganic elements. The
219 concentrations of trace metals (Pb, Ni, Zn, Cd) as well as Al and Fe and are significantly higher in the black river
220 and drainage canals than in the white river (Table 2, Figure 4). For Al, Fe and As, high concentrations are measured
221 in the black river during the first sampling campaign (drier conditions). In contrast to other TM, higher Cu
222 concentrations are measured in the white river. A PCA analysis (Figure 5) of TM concentration and DOM
223 properties reveals specific associations between DOC, Fe and As and to a lesser extent Zn and Cd, while another
224 group is formed by Al, Pb and Ni. Cu shows no association with DOM but does show increased concentrations
225 with higher FI. The first axis of PCA (load of DOC, Fe, As) strongly discriminates the black river and drainage
226 canals samples from the white river.

227 The distributions of DOC and TM are presented in Table 3. Dissolved organic carbon is mostly (>98%) dissolved
228 or in the form of fine colloids (<0.22 μm) along the entirety of the studied continuum. Iron and As are mostly
229 present in dissolved form or as fine colloids in the black river and drainage canals (>96%). However, after transfer
230 to the white river, half of Fe and a third of As is present in the coarse colloidal form. Zinc and Cd do not show
231 similar patterns. Aluminum is mostly present in the coarse colloidal phase (>60%) in the black river and drainage
232 canals and this proportion further increases in the white river (>80%). Lead is mostly present in the dissolved and
233 fine colloid phase (>75%) in the drainage canals and black river and shifts to coarse colloidal (>60%) forms after
234 the confluence with the white river. Nickel and Cu are mostly present in the dissolved and fine colloidal phase in
235 the DC and BR but almost entirely in the coarse colloidal fraction in the white river.

236 **5.4. Pb isotopic composition**

237 We observe distinct differences between the lead isotope ratios in the white river and those in the black river and
238 drainage canals. A decrease in the $^{206}\text{Pb}/^{207}\text{Pb}$ isotopic ratio is observed with increasing Pb concentrations in the
239 black river but not the white river (Figure 6a). Furthermore, the biplot of the $^{206}\text{Pb}/^{207}\text{Pb}$ and the $^{208}\text{Pb}/^{206}\text{Pb}$
240 signatures illustrates significant differences between the white water and black river/drainage canal groups (Figure
241 6b).

242 **6. Discussion**

243 **6.1. In-stream processing of DOM in black rivers**

244 We observe in-stream processing of DOM, but the total DOM exported from tropical peatlands exceeds the
245 processing capacity of the rivers which drain them and a large proportion of DOM is transported to the ocean. We
246 find persistently high DOC concentrations in both drainage canals and black rivers draining degraded peatlands
247 consistent with the range of previously reported values in Borneo (Cook et al., 2018; Moore et al., 2011) and in
248 the upper range of black rivers in Sumatra (Rixen et al., 2008; Baum et al., 2007). We also find indicators of in-
249 stream processing of DOM. The transformation of DOM we observe along the continuum is likely primarily due
250 to photo-oxidation with a smaller contribution from microbial processing. We observe an increase in the $\delta^{13}\text{C}$ -
251 DOC values along the studied continuum (Figure 3a). This shift toward higher $\delta^{13}\text{C}$ -DOC is correlated with an

252 increase in the C1/C2 ratio of PARAFAC fluorophores (Figure 3c). The two fluorophores are typical of terrestrial
253 input of DOM (Yamashita et al., 2008), and similar to observed fluorophores in other black rivers in Borneo
254 (Harun et al., 2015; Zhou et al., 2019). An increase in this C1/C2 ratio reflects a shift toward lower wavelengths
255 and therefore toward lower aromaticity and lower molecular weight (Austnes et al., 2010; Zhou et al., 2019).
256 Moreover, a decreasing trend in SUVA values is observed along the continuum (Figure 3b). These observations
257 indicate that at our site, aromatic features are preferentially processed in-stream, consistent with a dominant effect
258 of photo-oxidation (Amon and Benner, 1996; Sharpless et al., 2014; Spencer et al., 2009). This has also been
259 observed in the Congo River where photo-oxidation led to an increase in $\delta^{13}\text{C}$ -DOC and a decrease in aromatic
260 features (Spencer et al., 2009).

261 However, photo-oxidation is not the only process responsible for the processing of DOM. The low oxygen levels
262 in the black river and drainage canals and the significant relationship between DOC and DO concentrations suggest
263 that nearly all oxygen entering the well-mixed water is quickly consumed by DOM oxidation (Figure 2a&b).
264 Furthermore, the sharply decreasing oxygen profiles measured in the black river suggest that the transformation
265 of DOM is restricted to the shallow surface layers of these waters (Figure SI.3). Additionally, localized increases
266 in fluorescence index, coupled with decreases in SUVA (reflecting a higher proportion of microbial derived DOM,
267 Figure 3d) suggest that microbial processing occurs in some locations in drainage canals. Both photo-oxidation
268 and microbial processing have been quantified in laboratory experiments for DOM originating from tropical
269 peatlands. Martin et al. (2018) found that up to 25 % of riverine DOC from a black river in Sarawak, Malaysia,
270 was lost within 5 days of exposure to natural sunlight. Microbial long-term incubation studies by (Rixen et al.,
271 2008), showed that 27% of DOC was degraded after two weeks. In black rivers, it is likely that in-stream microbial
272 processing of DOM is limited by the low oxygen concentrations, low pH, and low nutrient levels (especially
273 inorganic nitrogen), (Wickland et al., 2012), rather than intrinsic refractory characteristics. Although the precise
274 extent of in-stream processing cannot be quantified here, our results are consistent with in stream transformation
275 of DOM by photo-oxidation as well as some contribution of microbial degradation in the shallow surface layers.
276 In the future, quantitative assessment of outgassing in tropical peatland drainage canals would improve the
277 evaluation of carbon release following peatland drainage. Overall, more work is needed to understand the extent
278 of upstream processing of peatland DOM.

279 **6.2. Role of DOM, Al and Fe in trace metal dynamics in peat draining waters**

280 This study provides the first record of trace metals in black rivers originating from degraded tropical peatlands.
281 We observe strong enrichment of Al and Fe, as well as Pb, As, Ni and Cd in peat-draining waters. The measured
282 concentrations are comparable to those measured by Kurasaki et al. (2000) in Borneo rivers for Pb, Zn, Cu and
283 Cd, but significantly higher (5 to 10 times) for Fe. The concentration levels, however, remain low compared to
284 highly impacted regions of Indonesia (Arifin et al., 2012). The elevated concentrations of Al and Fe in water
285 draining tropical peatlands is consistent with existing observations of elevated Fe concentrations from black rivers
286 in the tropics (Zhang et al., 2019) and northern peatlands. This enrichment is likely due to the weathering of mineral
287 material under the peat during peat accumulation processes (Tipping et al., 2002; Pokrovsky et al., 2005). As a
288 consequence, in water draining peatlands, strong organo-mineral associations between DOM and Fe (Krachler et
289 al. 2010, 2012; Broder and Biester 2015), as well as DOM and Al (Helmer et al., 1990) have been observed. These

290 colloidal associations between DOM and Al and Fe in the form of hydroxides strongly control TM transfer and
291 speciation in peat draining waters (Tipping et al., 2002). In the present study, specific associations of trace metals
292 with Al and Fe are observed, including strong links between Al and Pb and Ni. However, the lack of a direct
293 relationship between Pb and DOM contrasts with reported observations in the literature (Graham et al., 2006;
294 Jeremiason et al., 2018; Pokrovsky et al., 2016). Despite this, we do observe strong links between Fe, As, Zn, Cd
295 and DOM, which have been previously reported in water draining peatlands (Broder and Biester, 2015; Neubauer
296 et al., 2013; Pokrovsky et al., 2016). The coupled dynamics of Fe and As might be related to similar mobilization
297 processes within the peat column, with the sorption of As to Fe(III)-(oxyhydr)oxides (ThomasArrigo et al., 2014)
298 in anoxic peat water. Widespread drainage of tropical peatlands and the corresponding release of anoxic water to
299 surface water networks could induce a coupled increase in DOM and Fe concentrations, similar to that which has
300 occurred in Sweden (Kritzberg and Ekström, 2011).

301 **6.3. Peatlands as secondary sources of atmospheric pollutants**

302 The isotopic composition of Pb in peat draining water strongly suggests it is of anthropogenic origin. The isotopic
303 signatures measured in river samples are a combination of the signature of undisturbed soils of Borneo (Valentine
304 et al., 2008), and a mix of both present and past anthropogenic inputs. Older anthropogenic inputs are reflected by
305 the signature of atmospheric deposition from Java aerosols (Bollhöfer and Rosman, 2000), while the signature of
306 recent regional anthropogenic inputs was characterized by rain samples collected in Pontianak as part of this study
307 (Figure 6b). In the black river and drainage canals, the isotopic ratio is close to that of aerosols and recently sampled
308 rainwater and is dominated by anthropogenic inputs, whereas the isotopic ratio in the white river is closer to the
309 natural signal (Figure 6). This isotopic difference is consistent with the difference between the watersheds drained
310 by these two rivers: tropical peatlands are ombrotrophic systems, and the trace metal content in peat soil is derived
311 from the atmosphere (Weiss et al., 2002), whereas the Kapuas Kecil is recharged from a larger watershed and
312 reflects contribution of mineral soils. Tropical peatlands can serve as secondary sources of atmospheric pollutants
313 to the environment. With peatland drainage, black rivers release the accumulated atmospheric deposition over
314 hundreds of years on much shorter timescales. For example, the isotopic signature observed in the black river
315 reflects anthropogenic sources deposited at different times, including older deposition such as the lead measured
316 in the Java aerosols (Bollhöfer and Rosman, 2000), and more recent deposition following the widespread
317 introduction of unleaded fuel (characterized by samples collected from rainwater during the January 2014 sampling
318 period in this study). This release of lead by degraded tropical peatlands has the potential to impact records from
319 environmental archives, for example the corals of the Singapore Strait (Chen et al., 2015). Although this is the
320 first measurement of the aquatic release of trace metals from tropical peatlands, the role of tropical peatlands as a
321 secondary source of contaminants has also been highlighted by the trace metal content analysis of dust emitted to
322 the atmosphere by peat fires (Betha et al., 2013).

323 **6.4. From degraded tropical peatlands to the ocean**

324 Sharp changes in physico-chemical conditions are observed after the mixing of the black and the white river,
325 including sharp increases in DO concentrations and pH values. This strongly controls the transport of DOM and
326 TM drained from degraded tropical peatlands. After the confluence with the white river, DOC concentrations
327 decrease abruptly. This decrease primarily results from the dilution of the black river signal. However, the sudden

328 elevation of pH and DO after the confluence might create favorable conditions for microbial processing of DOC,
329 making the mixing zone a likely hotspot of GHG emissions (Palmer et al., 2016). This would also be consistent
330 with the decrease in the SUVA index observed after the confluence. Despite processing of DOM along the
331 continuum, a significant proportion of DOM originating from degraded peatlands actually reaches ocean. We
332 observe high DOC concentrations at all sampling locations, with concentrations remaining high even close to the
333 ocean (Figure 2a). Additionally, the results of our physical fractionation show that even close to the estuary, DOC
334 remains in the dissolved and fine colloid form ($<0.22 \mu\text{m}$), and that flocculation processes might be limited. The
335 large areas of coastal peatlands in the region might explain the relatively high fluvial organic carbon export to
336 South China Sea (Huang et al., 2017). The decrease in trace metal concentrations after the confluence might be
337 influenced by shifts in physical fractionation and an increased proportion of colloidal form. This is especially true
338 for Al and Pb. Some flocculation at the estuary might limit their transfer to the ocean. For Fe and As, a higher
339 proportion remains in the form of fine colloids after mixing with the whiter river, and is still associated with DOC.
340 Similar conservative behavior of LMW organic molecules associated with Fe was observed at the outlet of northern
341 peatlands (Krachler et al., 2012), and in Arctic rivers (Pokrovsky et al., 2014). This highlights that dissolved
342 organic molecules derived from tropical peatlands can also act as carriers of trace metals to the ocean.

343 **7. Conclusions**

344 This study characterizes the composition and concentration of DOM and TM in the canals and rivers draining the
345 degraded tropical peatlands of Indonesian Borneo. It highlights in-stream processing of DOM in drainage canals
346 and rivers draining degraded peatlands. Both stable isotopic and optical properties of DOM are consistent with
347 photo-oxidation along the continuum from the black river to the ocean. In the black river and drainage canals, rates
348 of microbial processing are likely limited to shallow depths. Along the continuum, DOM is found at relatively
349 high concentrations in the dissolved and fine colloidal phases, suggesting a substantial fraction of DOM derived
350 from degraded peatlands reaches the ocean. Additionally, we provide the first assessment of trace metal
351 concentrations in rivers draining degraded tropical peatlands. Rivers draining these peatlands are enriched in some
352 trace metals (Pb, Ni, Zn, Cd) as well as Al and Fe. Using the isotopic signature of Pb, we show that degraded
353 tropical peatlands are secondary sources of atmospherically deposited contaminants to surface waters. Trace metal
354 dynamics after transfer to the white river show clear trends: while Pb and Ni are associated with Al; As, Zn and
355 Cd are associated with Fe and DOM. Lead and Al are present in coarse colloidal form and may be transferred to
356 sediments after flocculation. In contrast, DOM, Fe and As are found predominantly in fine colloidal form even
357 after the confluence with the white river, and as a result may be transferred to the ocean. The role of degraded
358 tropical peatlands as a source of DOM, as well as Fe and As to the ocean requires further investigation.

359 **Author contribution**

360 LG, AMH, GH and CFH designed the study. LG, AMH, MN and GH conducted field campaigns. SM and LG
361 conducted fluorescence analysis. GLR and AC conducted lead isotope analysis. LG and AMH wrote the
362 manuscript, with inputs from all co-authors.

363 **Competing interests**

364 The authors declare no competing interests.

365 **Data availability**

366 The data are available at <https://doi.pangaea.de/10.1594/PANGAEA.909094>.

367 **Acknowledgements**

368 This research was supported by the National Research Foundation Singapore through the Singapore-MIT Alliance
369 for Research and Technology's Center for Environmental Sensing and Modeling interdisciplinary research
370 program and Grant No. NRF2016-ITCOO1-021, by the USA National Science Foundation under Grant No.
371 1923478 to C.F.H, and by the PEER project "Assessing Degradation of Tropical Peat Domes and Dissolved
372 Organic Carbon (DOC) Export from the Belait, Mempawah and Lower Kapuas Kecil Rivers in Borneo" lead by
373 G. A.. We thank F. Julien, V. Payre-Suc and D. Lambrigot for DOC and major elements analysis (PAPC platform,
374 EcoLab laboratory), and F. Candaudap for lead isotope analysis (ICP-MS platform, GET laboratory). We also
375 thank Patrick Martin and one anonymous reviewer for their constructive comments that improved the manuscript.

376 **References**

377 Alkhatib, M., Jennerjahn, T. C. and Samiaji, J.: Biogeochemistry of the Dumai River estuary, Sumatra, Indonesia,
378 a tropical black-water river, *Limnol. Oceanogr.*, 52(6), 2410–2417, doi:10.4319/lo.2007.52.6.2410, 2007.

379 Amon, R. M. W. and Benner, R.: Photochemical and microbial consumption of dissolved organic carbon and
380 dissolved oxygen in the Amazon River system, *Geochim. Cosmochim. Acta*, 60(10), 1783–1792,
381 doi:10.1016/0016-7037(96)00055-5, 1996.

382 Arifin, Z., Puspitasari, R. and Miyazaki, N.: Heavy metal contamination in Indonesian coastal marine ecosystems:
383 A historical perspective, *Coast. Mar. Sci.*, 35(1), 227–233, 2012.

384 Austnes, K., Evans, C. D., Eliot-Laize, C., Naden, P. S. and Old, G. H.: Effects of storm events on mobilisation
385 and in-stream processing of dissolved organic matter (DOM) in a Welsh peatland catchment, *Biogeochemistry*,
386 99(1), 157–173, doi:10.1007/s10533-009-9399-4, 2010.

387 Barber, A., Sirois, M., Chaillou, G. and Gélinas, Y.: Stable isotope analysis of dissolved organic carbon in
388 Canada's eastern coastal waters, *Limnol. Oceanogr.*, 62(S1), S71–S84, doi:10.1002/lno.10666, 2017.

389 Baum, A., Rixen, T. and Samiaji, J.: Relevance of peat draining rivers in central Sumatra for the riverine input of
390 dissolved organic carbon into the ocean, *Estuar. Coast. Shelf Sci.*, 73(3–4), 563–570,
391 doi:10.1016/j.ecss.2007.02.012, 2007.

392 Betha, R., Pradani, M., Lestari, P., Joshi, U. M., Reid, J. S. and Balasubramanian, R.: Chemical speciation of trace
393 metals emitted from Indonesian peat fires for health risk assessment, *Atmospheric Res.*, 122(Supplement C), 571–
394 578, doi:10.1016/j.atmosres.2012.05.024, 2013.

395 Bollhöfer, A. and Rosman, K. J. R.: Isotopic source signatures for atmospheric lead: the Southern Hemisphere,
396 *Geochim. Cosmochim. Acta*, 64(19), 3251–3262, doi:10.1016/S0016-7037(00)00436-1, 2000.

397 Bro, R.: PARAFAC. Tutorial and applications - ScienceDirect, *Chemom. Intell. Lab. Syst.*, 149–171, 1997.

398 Broder, T. and Biester, H.: Hydrologic controls on DOC, As and Pb export from a polluted peatland – the
399 importance of heavy rain events, antecedent moisture conditions and hydrological connectivity, *Biogeosciences*,
400 12(15), 4651–4664, doi:<https://doi.org/10.5194/bg-12-4651-2015>, 2015.

401 Broder, T. and Biester, H.: Linking major and trace element concentrations in a headwater stream to DOC release
402 and hydrologic conditions in a bog and peaty riparian zone, *Appl. Geochem.*, 87, 188–201,
403 doi:10.1016/j.apgeochem.2017.11.003, 2017.

404 Carlson, K. M., Goodman, L. K. and May-Tobin, C. C.: Modeling relationships between water table depth and
405 peat soil carbon loss in Southeast Asian plantations, *Environ. Res. Lett.*, 10(7), 074006, doi:10.1088/1748-
406 9326/10/7/074006, 2015.

407 Chen, M., Lee, J.-M., Nurhati, I. S., Switzer, A. D. and Boyle, E. A.: Isotopic record of lead in Singapore Straits
408 during the last 50 years: Spatial and temporal variations, *Mar. Chem.*, 168, 49–59,
409 doi:10.1016/j.marchem.2014.10.007, 2015.

410 Cobb, A. R., Hoyt, A. M., Gandois, L., Eri, J., Dommain, R., Salim, K. A., Kai, F. M., Su'ut, N. S. H. and Harvey,
411 C. F.: How temporal patterns in rainfall determine the geomorphology and carbon fluxes of tropical peatlands,
412 *Proc. Natl. Acad. Sci.*, 114(26), E5187–E5196, doi:10.1073/pnas.1701090114, 2017.

413 Cook, S., Whelan, M. J., Evans, C. D., Gauci, V., Peacock, M., Garnett, M. H., Kho, L. K., Teh, Y. A. and Page,
414 S. E.: Fluvial organic carbon fluxes from oil palm plantations on tropical peatland, *Biogeosciences*, 15(24), 7435–
415 7450, doi:https://doi.org/10.5194/bg-15-7435-2018, 2018.

416 Cory, R. M., Miller, M. P., McKnight, D. M., Guerard, J. J. and Miller, P. L.: Effect of instrument-specific response
417 on the analysis of fulvic acid fluorescence spectra, *Limnol. Oceanogr. Methods*, 8(2), 67–78,
418 doi:10.4319/lom.2010.8.67, 2010.

419 Couwenberg, J., Dommain, R. and Joosten, H.: Greenhouse gas fluxes from tropical peatlands in south-east Asia,
420 *Glob. Change Biol.*, 16(6), 1715–1732, doi:10.1111/j.1365-2486.2009.02016.x, 2010.

421 Dargie, G. C., Lewis, S. L., Lawson, I. T., Mitchard, E. T. A., Page, S. E., Bocko, Y. E. and Ifo, S. A.: Age, extent
422 and carbon storage of the central Congo Basin peatland complex, *Nature*, 542(7639), 86–90,
423 doi:10.1038/nature21048, 2017.

424 Dinno, A.: dunn.test: Dunn's Test of Multiple Comparisons Using Rank Sums. R package version 1.3.5.
425 <https://CRAN.R-project.org/package=dunn.test>, 2017.

426 Fellman, J. B., Miller, M. P., Cory, R. M., D'Amore, D. V. and White, D.: Characterizing Dissolved Organic
427 Matter Using PARAFAC Modeling of Fluorescence Spectroscopy: A Comparison of Two Models, *Environ. Sci.*
428 *Technol.*, 43(16), 6228–6234, doi:10.1021/es900143g, 2009.

429 Gandois, L., Cobb, A. R., Hei, I. C., Lim, L. B. L., Salim, K. A. and Harvey, C. F.: Impact of deforestation on
430 solid and dissolved organic matter characteristics of tropical peat forests: implications for carbon release,
431 *Biogeochemistry*, 114(1), 183–199, doi:10.1007/s10533-012-9799-8, 2013.

432 Gandois, L., Teisserenc, R., Cobb, A. R., Chieng, H. I., Lim, L. B. L., Kamariah, A. S., Hoyt, A. and Harvey, C.
433 F.: Origin, composition, and transformation of dissolved organic matter in tropical peatlands, *Geochim.*
434 *Cosmochim. Acta*, 137, 35–47, doi:10.1016/j.gca.2014.03.012, 2014.

435 Graham, M. C., Vinogradoff, S. I., Chipchase, A. J., Dunn, S. M., Bacon, J. R. and Farmer, J. G.: Using Size
436 Fractionation and Pb Isotopes to Study Pb Transport in the Waters of an Organic-Rich Upland Catchment, *Environ.*
437 *Sci. Technol.*, 40(4), 1250–1256, doi:10.1021/es0517670, 2006.

438 Hansen, A. M., Kraus, T. E. C., Pellerin, B. A., Fleck, J. A., Downing, B. D. and Bergamaschi, B. A.: Optical
439 properties of dissolved organic matter (DOM): Effects of biological and photolytic degradation, *Limnol.*
440 *Oceanogr.*, 61(3), 1015–1032, doi:10.1002/lno.10270, 2016.

441 Harun, S., Baker, A., Bradley, C., Pinay, G., Boomer, I. and Liz Hamilton, R.: Characterisation of dissolved
442 organic matter in the Lower Kinabatangan River, Sabah, Malaysia, *Hydrol. Res.*, 46(3), 411–428,
443 doi:10.2166/nh.2014.196, 2015.

444 Helmer, E. H., Urban, N. R. and Eisenreich, S. J.: Aluminum geochemistry in peatland waters, *Biogeochemistry*,
445 9(3), doi:10.1007/BF00000601, 1990.

- 446 Hood, E., Williams, M. W. and McKnight, D. M.: Sources of dissolved organic matter (DOM) in a Rocky
447 Mountain stream using chemical fractionation and stable isotopes, *Biogeochemistry*, 74(2), 231–255,
448 doi:10.1007/s10533-004-4322-5, 2005.
- 449 Hooijer, A., Page, S., Jauhiainen, J., Lee, W. A., Lu, X. X., Idris, A. and Anshari, G.: Subsidence and carbon loss
450 in drained tropical peatlands, *Biogeosciences*, 9(3), 1053–1071, doi:10.5194/bg-9-1053-2012, 2012.
- 451 Hoyt, A. M., Gandois, L., Eri, J., Kai, F. M., Harvey, C. F. and Cobb, A. R.: CO₂ emissions from an undrained
452 tropical peatland: Interacting influences of temperature, shading and water table depth, *Glob. Change Biol.*, 25(9),
453 2885–2899, doi:10.1111/gcb.14702, 2019.
- 454 Huang, T. H., Chen, C. T. A., Tseng, H. C., Lou, J. Y., Wang, S. L., Yang, L., Kandasamy, S., Gao, X., Wang, J.
455 T., Aldrian, E., Jacinto, G. S., Anshari, G. Z., Sompongchaiyakul, P. and Wang, B. J.: Riverine carbon fluxes to
456 the South China Sea, *J. Geophys. Res. Biogeosciences*, 122(5), 1239–1259, doi:10.1002/2016JG003701, 2017.
- 457 Jaffé, R., McKnight, D., Maie, N., Cory, R., McDowell, W. H. and Campbell, J. L.: Spatial and temporal variations
458 in DOM composition in ecosystems: The importance of long-term monitoring of optical properties, *J. Geophys.*
459 *Res. Biogeosciences*, 113(G4), doi:10.1029/2008JG000683, 2008.
- 460 Jauhiainen, J., Hooijer, A. and Page, S. E.: Carbon Dioxide emissions from an Acacia plantation on peatland in
461 Sumatra, Indonesia, , doi:https://doi.org/10.5194/bg-9-617-2012, 2012.
- 462 Jeremiason, J. D., Baumann, E. I., Sebestyen, S. D., Agather, A. M., Seelen, E. A., Carlson-Stehlin, B. J., Funke,
463 M. M. and Cotner, J. B.: Contemporary Mobilization of Legacy Pb Stores by DOM in a Boreal Peatland, *Environ.*
464 *Sci. Technol.*, 52(6), 3375–3383, doi:10.1021/acs.est.7b06577, 2018.
- 465 Krachler, M., Roux, G. L., Kober, B. and Shotyk, W.: Optimising accuracy and precision of lead isotope
466 measurement (206 Pb, 207 Pb, 208 Pb) in acid digests of peat with ICP-SMS using individual mass discrimination
467 correction, *J. Anal. At. Spectrom.*, 19(3), 354–361, doi:10.1039/B314956K, 2004.
- 468 Krachler, R., Krachler, R. F., von der Kammer, F., Süphandag, A., Jirsa, F., Ayromlou, S., Hofmann, T. and
469 Keppler, B. K.: Relevance of peat-draining rivers for the riverine input of dissolved iron into the ocean, *Sci. Total*
470 *Environ.*, 408(11), 2402–2408, doi:10.1016/j.scitotenv.2010.02.018, 2010.
- 471 Krachler, R., von der Kammer, F., Jirsa, F., Süphandag, A., Krachler, R. F., Plessl, C., Vogt, M., Keppler, B. K.
472 and Hofmann, T.: Nanoscale lignin particles as sources of dissolved iron to the ocean: NANOSCALE LIGNIN
473 PARTICLES, *Glob. Biogeochem. Cycles*, 26(3), n/a-n/a, doi:10.1029/2012GB004294, 2012.
- 474 Kritzberg, E. S. and Ekström, S. M.: Increasing iron concentrations in surface waters – a factor behind
475 brownification?, *Biogeosciences Discuss.*, 8(6), 12285–12316, doi:10.5194/bgd-8-12285-2011, 2011.
- 476 Kurasaki, M., Hartoto, D. I., Saito, T., Suzuki-Kurasaki, M. and Iwakuma, T.: Metals in Water in the Central
477 Kalimantan, Indonesia, *Bull. Environ. Contam. Toxicol.*, 65(5), 591–597, doi:10.1007/s0012800164, 2000.
- 478 Lähteenoja, O., Ruokolainen, K., Schulman, L. and Oinonen, M.: Amazonian peatlands: an ignored C sink and
479 potential source, *Glob. Change Biol.*, 15(9), 2311–2320, doi:10.1111/j.1365-2486.2009.01920.x, 2009.
- 480 Lalonde, K., Vähätalo, A. and Gélinas, Y.: Revisiting the disappearance of terrestrial dissolved organic matter in
481 the ocean: a $\delta^{13}\text{C}$ study, *Biogeosciences*, 11(13) [online] Available from:
482 <https://jyx.jyu.fi/handle/123456789/44281> (Accessed 16 June 2019), 2014.
- 483 Luciani, X., Mounier, S., Paraquetti, H. H. M., Redon, R., Lucas, Y., Bois, A., Lacerda, L. D., Raynaud, M. and
484 Ripert, M.: Tracing of dissolved organic matter from the SEPETIBA Bay (Brazil) by PARAFAC analysis of total
485 luminescence matrices, *Mar. Environ. Res.*, 65(2), 148–157, doi:10.1016/j.marenvres.2007.09.004, 2008.
- 486 Luciani, X., Mounier, S., Redon, R. and Bois, A.: A simple correction method of inner filter effects affecting
487 FEEM and its application to the PARAFAC decomposition, *Chemom. Intell. Lab. Syst.*, 96(2), 227–238,
488 doi:10.1016/j.chemolab.2009.02.008, 2009.

- 489 Martin, P., Cherukuru, N., Tan, A. S. Y., Sanwlani, N., Mujahid, A. and Müller, M.: Distribution and cycling of
490 terrigenous dissolved organic carbon in peatland-draining rivers and coastal waters of Sarawak, Borneo, ,
491 doi:<http://dx.doi.org/10.5194/bg-15-6847-2018>, 2018.
- 492 McKnight, D. M., Boyer, E. W., Westerhoff, P. K., Doran, P. T., Kulbe, T. and Andersen, D. T.:
493 Spectrofluorometric characterization of dissolved organic matter for indication of precursor organic material and
494 aromaticity, *Limnol. Oceanogr.*, 46(1), 38–48, doi:10.4319/lo.2001.46.1.0038, 2001.
- 495 Miettinen, J., Hooijer, A., Vernimmen, R., Liew, S. C. and Page, S. E.: From carbon sink to carbon source:
496 extensive peat oxidation in insular Southeast Asia since 1990, *Environ. Res. Lett.*, 12(2), 024014,
497 doi:10.1088/1748-9326/aa5b6f, 2017.
- 498 Moore, S., Gauci, V., Evans, C. D. and Page, S. E.: Fluvial organic carbon losses from a Bornean blackwater river,
499 *Biogeosciences*, 8, 901–909, 2011.
- 500 Moore, S., Evans, C. D., Page, S. E., Garnett, M. H., Jones, T. G., Freeman, C., Hooijer, A., Wiltshire, A. J., Limin,
501 S. H. and Gauci, V.: Deep instability of deforested tropical peatlands revealed by fluvial organic carbon fluxes,
502 *Nature*, 493(7434), 660–663, doi:10.1038/nature11818, 2013.
- 503 Müller, D., Warneke, T., Rixen, T., Müller, M., Jamahari, S., Denis, N., Mujahid, A. and Notholt, J.: Lateral carbon
504 fluxes and CO₂ outgassing from a tropical peat-draining river, *Biogeosciences Discuss.*,
505 12(13), 10389–10424, doi:10.5194/bgd-12-10389-2015, 2015.
- 506 Neubauer, E., von der Kammer, F., Knorr, K.-H., Peiffer, S., Reichert, M. and Hofmann, T.: Colloid-associated
507 export of arsenic in stream water during stormflow events, *Chem. Geol.*, 352, 81–91,
508 doi:10.1016/j.chemgeo.2013.05.017, 2013.
- 509 Page, S. E., Rieley, J. O. and Wüst, R.: Chapter 7 Lowland tropical peatlands of Southeast Asia, in *Developments*
510 *in Earth Surface Processes*, vol. 9, edited by I. P. Martini, A. Martínez Cortizas, and W. Chesworth, pp. 145–172,
511 Elsevier., 2006.
- 512 Page, S. E., Rieley, J. O. and Banks, C. J.: Global and regional importance of the tropical peatland carbon pool,
513 *Glob. Change Biol.*, 17(2), 798–818, doi:10.1111/j.1365-2486.2010.02279.x, 2011.
- 514 Palmer, S. M., Evans, C. D., Chapman, P. J., Burden, A., Jones, T. G., Allott, T. E. H., Evans, M. G., Moody, C.
515 S., Worrall, F. and Holden, J.: Sporadic hotspots for physico-chemical retention of aquatic organic carbon: from
516 peatland headwater source to sea, *Aquat. Sci.*, 78(3), 491–504, doi:10.1007/s00027-015-0448-x, 2016.
- 517 Pokrovsky, O. S., Dupré, B. and Schott, J.: Fe–Al–organic Colloids Control of Trace Elements in Peat Soil
518 Solutions: Results of Ultrafiltration and Dialysis, *Aquat. Geochem.*, 11(3), 241–278, doi:10.1007/s10498-004-
519 4765-2, 2005.
- 520 Pokrovsky, O. S., Shirokova, L. S., Viers, J., Gordeev, V. V., Shevchenko, V. P., Chupakov, A. V., Vorobieva, T.
521 Y., Candaudap, F., Causserand, C., Lanzasova, A. and Zouiten, C.: Fate of colloids during estuarine mixing in the
522 Arctic, *Ocean Sci.*, 10(1), 107–125, doi:10.5194/os-10-107-2014, 2014.
- 523 Pokrovsky, O. S., Manasypov, R. M., Loiko, S. V. and Shirokova, L. S.: Organic and organo-mineral colloids in
524 discontinuous permafrost zone, *Geochim. Cosmochim. Acta*, 188, 1–20, doi:10.1016/j.gca.2016.05.035, 2016.
- 525 Poulin, B. A., Ryan, J. N. and Aiken, G. R.: Effects of Iron on Optical Properties of Dissolved Organic Matter,
526 *Environ. Sci. Technol.*, 48(17), 10098–10106, doi:10.1021/es502670r, 2014.
- 527 R Core Team: A language and environment for statistical computing, R Foundation for Statistical Computing,
528 Vienna, Austria (<http://R-project.org/>), 2019.
- 529 Rixen, T., Baum, A., Pohlmann, T., Balzer, W., Samiaji, J. and Jose, C.: The Siak, a tropical black water river in
530 central Sumatra on the verge of anoxia, *Biogeochemistry*, 90(2), 129–140, doi:10.1007/s10533-008-9239-y, 2008.

- 531 Rothwell, J. J., Evans, M. G., Daniels, S. M. and Allott, T. E. H.: Baseflow and stormflow metal concentrations in
532 streams draining contaminated peat moorlands in the Peak District National Park (UK), *J. Hydrol.*, 341(1), 90–
533 104, doi:10.1016/j.jhydrol.2007.05.004, 2007.
- 534 Rothwell, J. J., Evans, M. G., Daniels, S. M. and Allott, T. E. H.: Peat soils as a source of lead contamination to
535 upland fluvial systems, *Environ. Pollut.*, 153(3), 582–589, doi:10.1016/j.envpol.2007.09.009, 2008.
- 536 Sharpless, C. M., Aeschbacher, M., Page, S. E., Wenk, J., Sander, M. and McNeill, K.: Photooxidation-Induced
537 Changes in Optical, Electrochemical, and Photochemical Properties of Humic Substances, *Environ. Sci. Technol.*,
538 48(5), 2688–2696, doi:10.1021/es403925g, 2014.
- 539 Spencer, R. G. M., Stubbins, A., Hernes, P. J., Baker, A., Mopper, K., Aufdenkampe, A. K., Dyda, R. Y., Mwamba,
540 V. L., Mangangu, A. M., Wabakanghanzi, J. N. and Six, J.: Photochemical degradation of dissolved organic matter
541 and dissolved lignin phenols from the Congo River, *J. Geophys. Res. Biogeosciences*, 114(G3),
542 doi:10.1029/2009JG000968, 2009.
- 543 ThomasArrigo, L. K., Mikutta, C., Byrne, J., Barmettler, K., Kappler, A. and Kretzschmar, R.: Iron and Arsenic
544 Speciation and Distribution in Organic Flocs from Streambeds of an Arsenic-Enriched Peatland, *Environ. Sci.*
545 *Technol.*, 48(22), 13218–13228, doi:10.1021/es503550g, 2014.
- 546 Tipping, E., Rey-Castro, C., Bryan, S. E. and Hamilton-Taylor, J.: Al(III) and Fe(III) binding by humic substances
547 in freshwaters, and implications for trace metal speciation, *Geochim. Cosmochim. Acta*, 66(18), 3211–3224,
548 doi:10.1016/S0016-7037(02)00930-4, 2002.
- 549 Valentine, B., Kamenov, G. D. and Krigbaum, J.: Reconstructing Neolithic groups in Sarawak, Malaysia through
550 lead and strontium isotope analysis, *J. Archaeol. Sci.*, 35(6), 1463–1473, doi:10.1016/j.jas.2007.10.016, 2008.
- 551 Weishaar, J. L., Aiken, G. R., Bergamaschi, B. A., Fram, M. S., Fujii, R. and Mopper, K.: Evaluation of Specific
552 Ultraviolet Absorbance as an Indicator of the Chemical Composition and Reactivity of Dissolved Organic Carbon,
553 *Environ. Sci. Technol.*, 37(20), 4702–4708, doi:10.1021/es030360x, 2003.
- 554 Weiss, D., Shotyk, W., Rieley, J., Page, S., Gloor, M., Reese, S. and Martinez-Cortizas, A.: The geochemistry of
555 major and selected trace elements in a forested peat bog, Kalimantan, SE Asia, and its implications for past
556 atmospheric dust deposition, *Geochim. Cosmochim. Acta*, 66(13), 2307–2323, doi:10.1016/S0016-
557 7037(02)00834-7, 2002.
- 558 Wickham, H.: *ggplot2: Elegant Graphics for Data Analysis.*, 2016.
- 559 Wickham, H., François, R., Henry, L. and Müller, K.: *dplyr: A Grammar of Data Manipulation.* R package version
560 0.8.0.1. <https://CRAN.R-project.org/package=dplyr>, 2019.
- 561 Wickland, K. P., Aiken, G. R., Butler, K., Dornblaser, M. M., Spencer, R. G. M. and Striegl, R. G.:
562 Biodegradability of dissolved organic carbon in the Yukon River and its tributaries: Seasonality and importance
563 of inorganic nitrogen, *Glob. Biogeochem. Cycles*, doi:10.1029/2012GB004342@10.1002/(ISSN)1944-
564 9224.AQUNETWRK1, 2012.
- 565 Wit, F., Müller, D., Baum, A., Warneke, T., Pranowo, W. S., Müller, M. and Rixen, T.: The impact of disturbed
566 peatlands on river outgassing in Southeast Asia, *Nat. Commun.*, 6, 10155, doi:10.1038/ncomms10155, 2015.
- 567 Yamashita, Y., Jaffé, R., Maie, N. and Tanoue, E.: Assessing the dynamics of dissolved organic matter (DOM) in
568 coastal environments by excitation emission matrix fluorescence and parallel factor analysis (EEM-PARAFAC),
569 *Limnol. Oceanogr.*, 53(5), 1900–1908, doi:10.4319/lo.2008.53.5.1900, 2008.
- 570 Zhang, X., Müller, M., Jiang, S., Wu, Y., Zhu, X., Mujahid, A., Zhu, Z., Muhamad, M. F., Sia, E. S. A., Jang, F.
571 H. A. and Zhang, J.: Distribution and Flux of Dissolved Iron of the Rajang and Blackwater Rivers at Sarawak,
572 Borneo, *Biogeosciences Discuss.*, 1–31, doi:<https://doi.org/10.5194/bg-2019-204>, 2019.
- 573 Zhou, Y., Martin, P. and Müller, M.: Composition and cycling of dissolved organic matter from tropical peatlands
574 of coastal Sarawak, Borneo, revealed by fluorescence spectroscopy and parallel factor analysis, *Biogeosciences*,
575 16(13), 2733–2749, doi:10.5194/bg-16-2733-2019, 2019.

577

578 **Table 1.** Mean and standard deviation (mean±sd) of pH, conductivity and main elemental concentrations of the white river, upstream of the white river, black river and drainage
579 canals for the two sampling campaigns (June: drier period, January, wetter period). DO: Dissolved oxygen, FI: Fluorescence Index, SUVA: Specific UV Absorbance).

		n	pH /	DO mg L ⁻¹	Cond μS cm ⁻¹	SM mg L ⁻¹	DOC mg L ⁻¹	N-NO ₃ μmol L ⁻¹	N-NH ₄ μmol L ⁻¹	P-PO ₄ μmol L ⁻¹	Cl ⁻ mg.L ⁻¹	δ ¹³ DOC ‰	FI -	SUVA L.mg ⁻¹ .m ⁻¹
White River	dry	5	5.2 ± 0.33	4.49 ± 0.26	37.2 ± 13.2	47.9 ± 13.2	8.43 ± 1.61	0.192 ± 0.062	<DL	<DL	4.83 ± 4.03	-29.46 ± 0.23	1.63 ± 0.08	3.4 ± 0
	wet	5	4.43 ± 0.86	3.37 ± 0.96	1220.6 ± 981.8	21.1 ± 2.5	11.25 ± 4.29	0.043 ± 0.049	<DL	0.003 ± 0.249	409 ± 342	-29.41 ± 0.41	1.64 ± 0.04	4.6 ± 0.3
White River upstream	dry	2	5.45 ± 5.71	4.91 ± 0.17	24 ± 3.8	55.7 ± 17.2	6.89 ± 1.28	0.196 ± 0.033	<DL	<DL	1.31 ± 0.64	-29.32 ± 0.06	1.54 ± 0	n.a
	wet	3	5.37 ± 0.06	4.15 ± 0.39	268.7 ± 92	29.4 ± 10.1	8.69 ± 0.78	0.061 ± 0.011	<DL	0.005 ± 0.404	47.9 ± 65.2	-29.56 ± 0.13	1.57 ± 0.01	4.1 ± 0.1
Black river	dry	8	3.45 ± 0.06	1.69 ± 0.39	98.7 ± 18.2	23.7 ± 19.1	36.42 ± 2.54	0.092 ± 0.042	0.120 ± 0.091	0.023 ± 2.32	2.78 ± 0.5	-30.29 ± 0.38	1.7 ± 0.04	4.8 ± 0.4
	wet	11	2.97 ± 0.13	1.98 ± 0.75	77.3 ± 18.3	13.4 ± 8.5	35.37 ± 3.7	0.043 ± 0.022	0.014 ± 0.028	0.014 ± 1.22	2.2 ± 0.6	-30.04 ± 0.38	1.8 ± 0.09	4.9 ± 1.3
Drainage canal	wet	6	3.08 ± 0.43	2.34 ± 0.3	89.8 ± 19.6	n.a	35.17 ± 5.47	0.034 ± 0.033	0.020 ± 0.039	0.021 ± 1.65	2.6 ± 0.6	-30.27 ± 0.4	1.8 ± 0.13	4.3 ± 1.3

580

581 **Table 2.** Mean and standard deviation (mean±sd) of trace metal concentration of the white river, white river tributaries, black river and drainage canals for the two sampling
582 campaigns (June: drier period, January, wetter period).

		n	Al μg.L ⁻¹	Fe μg.L ⁻¹	Pb μg.L ⁻¹	As μg.L ⁻¹	Ni μg.L ⁻¹	Zn μg.L ⁻¹	Cu μg.L ⁻¹	Ni μg.L ⁻¹	Cd μg.L ⁻¹
White River	dry	5	312 ± 407.1	444.9 ± 383.9	0.262 ± 0.236	0.276 +/- 0.093	0.53 ± 0.11	18.57 ± 9.028	1.14 ± 0.16	0.53 ± 0.11	0.005 +/- 0.002
	wet	5	147.2 ± 124.6	547.5 ± 497.3	0.129 ± 0.102	0.322 +/- 0.094	1.19 ± 1.17	10.26 ± 6.14	0.87 ± 0.09	1.19 ± 1.17	0.006 +/- 0.003
White River upstream.	dry	2	101.61 ± 27.5	242.5 ± 44.5	0.139 ± 0.027	0.213 +/- 0.016	0.52 ± 0.08	15.29 ± 3.06	1.06 ± 0.01	0.52 ± 0.08	0.003 +/- 0.000
	wet	3	148.6 ± 72	408.7 ± 170.2	0.236 ± 0.167	0.299 +/- 0.038	0.72 ± 0.44	9.7 ± 6.23	1.19 ± 0.24	0.72 ± 0.44	0.003 +/- 0.000
Black river	dry	8	592.8 ± 43	2143.5 ± 187.6	0.467 ± 0.054	0.591 +/- 0.044	1.96 ± 1.67	119.38 ± 86.47	0.58 ± 0.19	1.96 ± 1.67	0.012 +/- 0.006
	wet	11	443.1 ± 137.5	1441 ± 493.5	0.316 ± 0.11	0.398 +/- 0.1	1.3 ± 0.53	10.95 ± 6.98	0.72 ± 1.13	1.3 ± 0.53	0.007 +/- 0.003
Drainage canal	wet	6	489.2 ± 194.9	1348 ± 494.1	0.313 ± 0.048	0.353 +/- 0.078	1.54 ± 0.8	14.52 ± 11.62	0.37 ± 0.07	1.54 ± 0.8	0.008 +/- 0.006

583

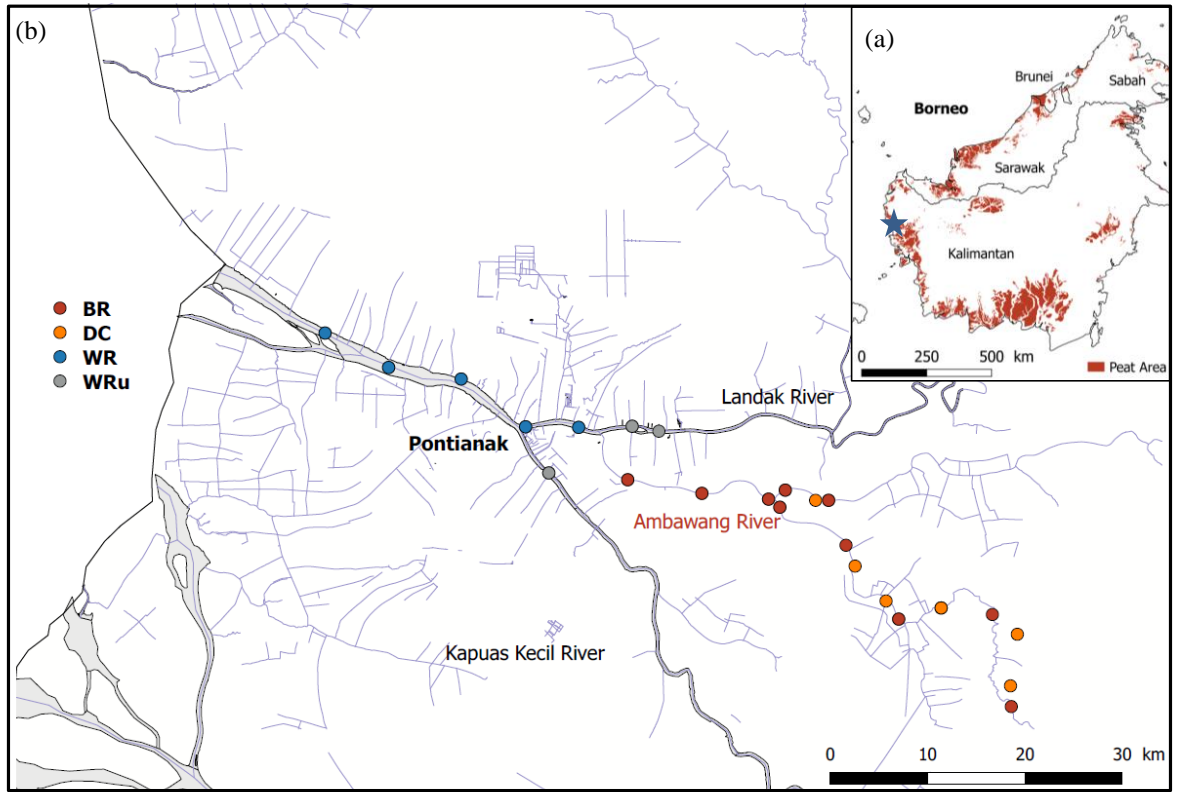
584 **Table 3.** Proportion of DOC and selected trace metals in the form of dissolved and fine colloids (< 0.22 μm) and
 585 coarse colloids (0.2-2.7 μm)

586

	Drainage Canals		Black River		White River	
	<0.2 μm	0.2-2.7 μm	<0.2 μm	0.2-2.7 μm	<0.2 μm	0.2-2.7 μm
DOC	97	3	98	2	100	0
Al	39	61	36	64	18	82
Fe	100	0	99	1	45	55
Pb	75	25	78	22	34	66
As	98	2	96	4	67	33
Ni	72	28	50	50	1	99
Cu	68	32	48	52	1	99
Zn	13	87	12	88	26	74
Cd	66	34	100	0	83	17

587

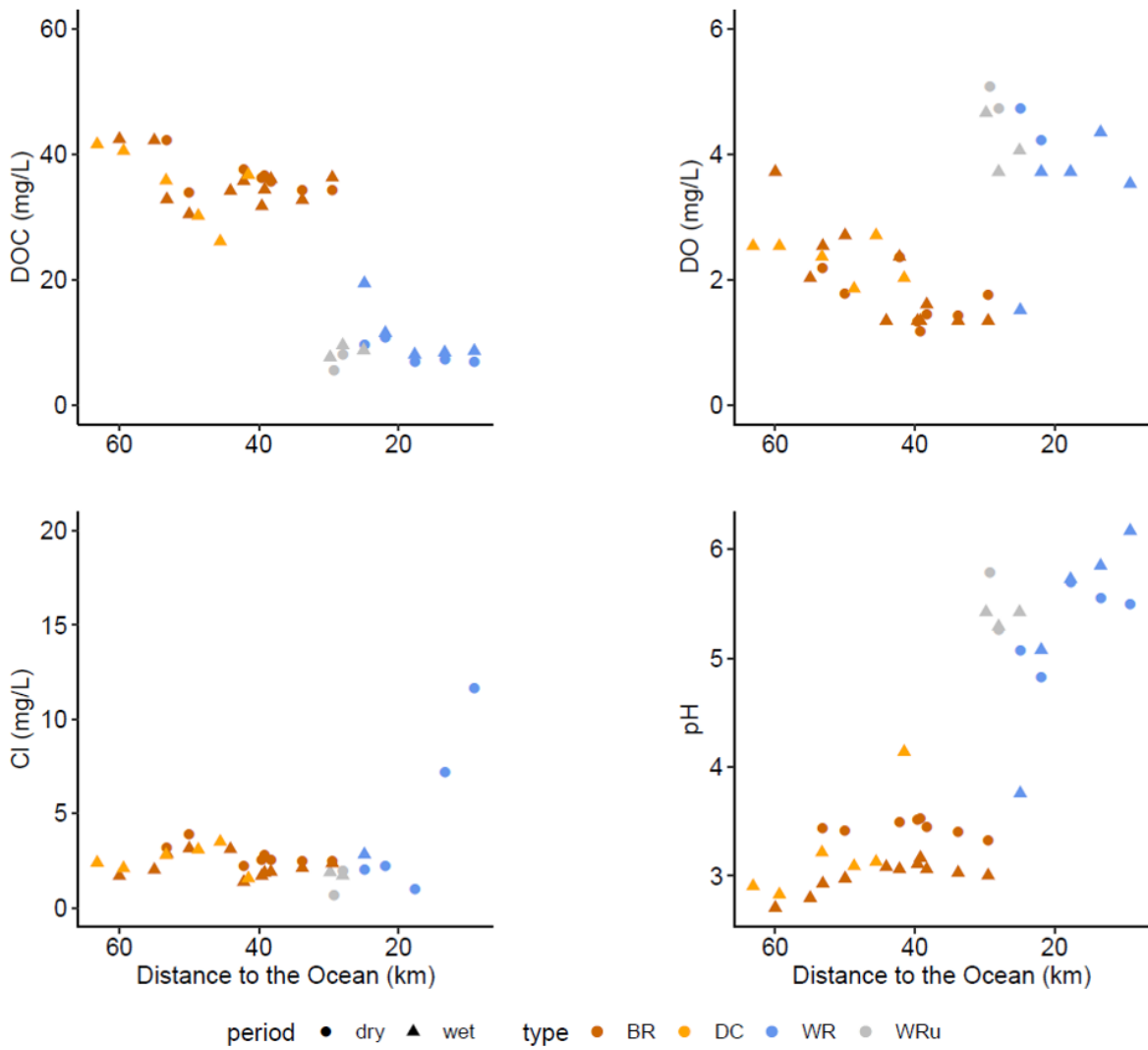
588
589
590
591



592
593
594
595
596
597
598

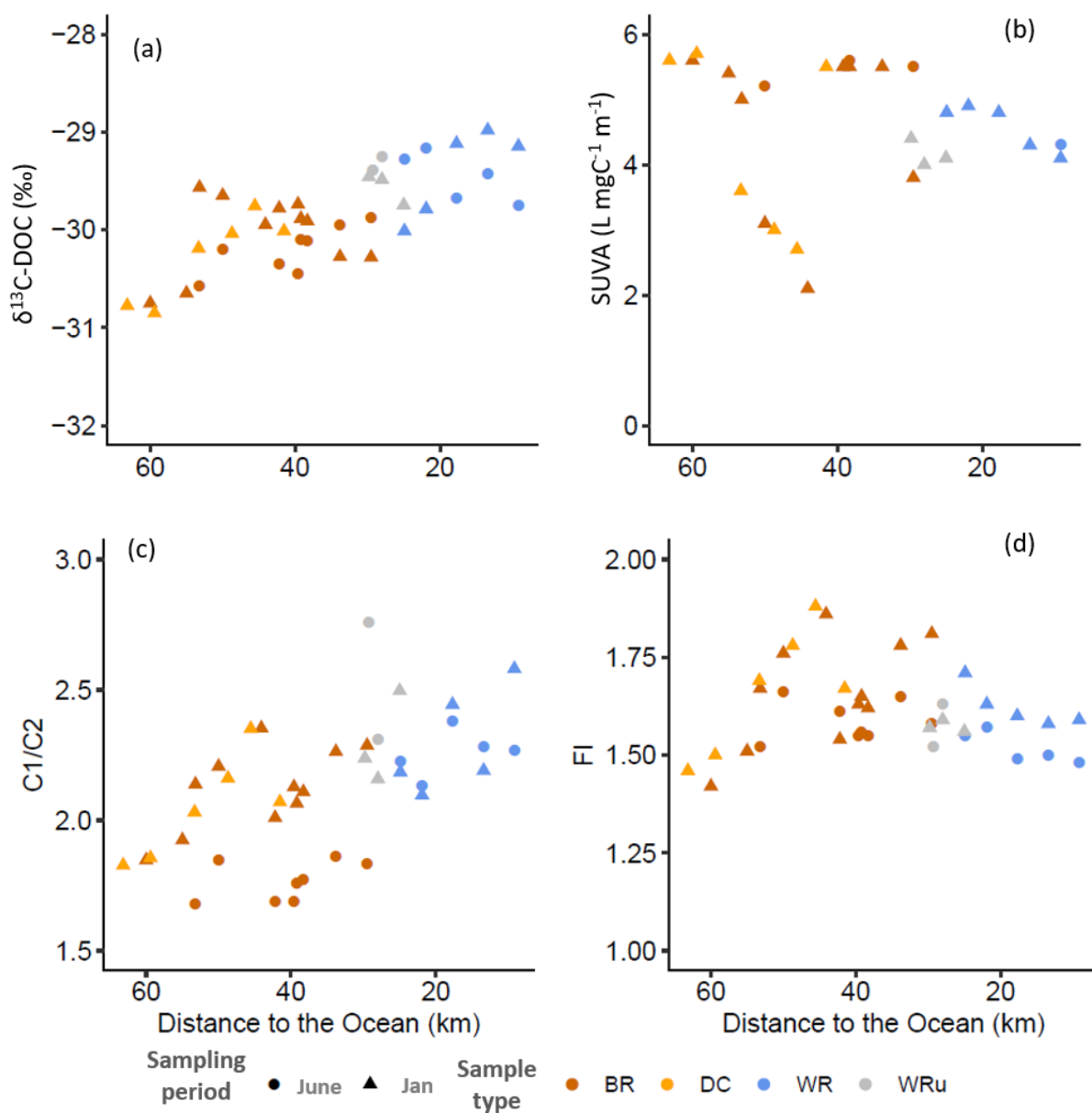
Figure 1: (a) Location of the study area on Borneo island. (b) Location of sampling sites and types of water: Black River (BR). Drainage Canals (DC). White River (WR). and white River upstream of the confluence with the black river (WRu).

599
600
601
602
603
604
605



606
607
608
609
610
611
612

Figure 2: Evolution of (a) dissolved organic carbon (DOC) concentration. (b) dissolved oxygen (DO) concentration. (c) chloride concentration and (d) pH along the continuum from the black river to the ocean.

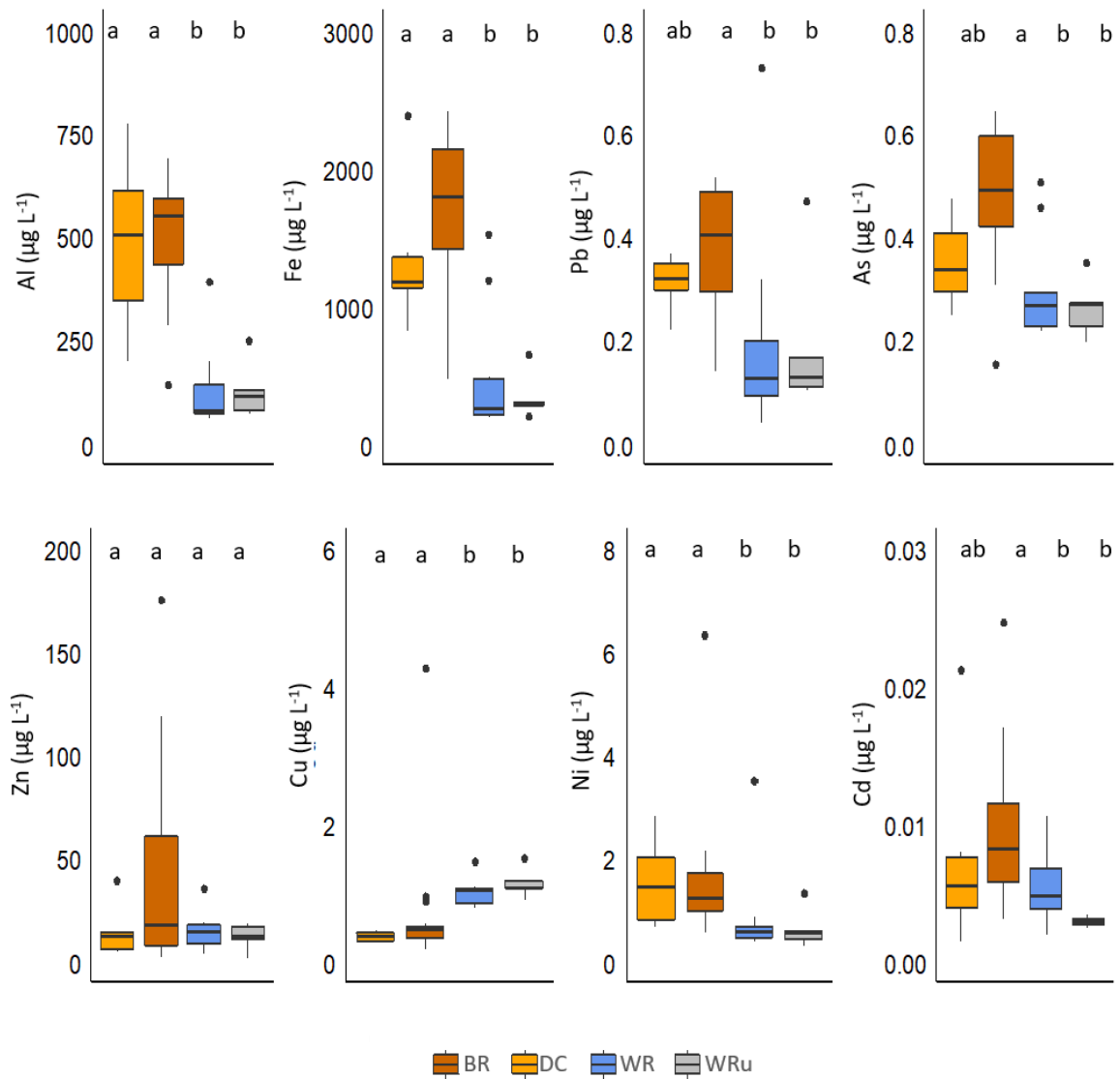


614

615

616 **Figure 3:** Evolution of DOM along the black river to the ocean continuum. (a) $\delta^{13}\text{C-DOC}$. (b) SUVA (Specific
 617 UV Absorbance) index. (c) C1/C2. (d) FI (Fluorescence Index).

618



619

620

621

622

623

624

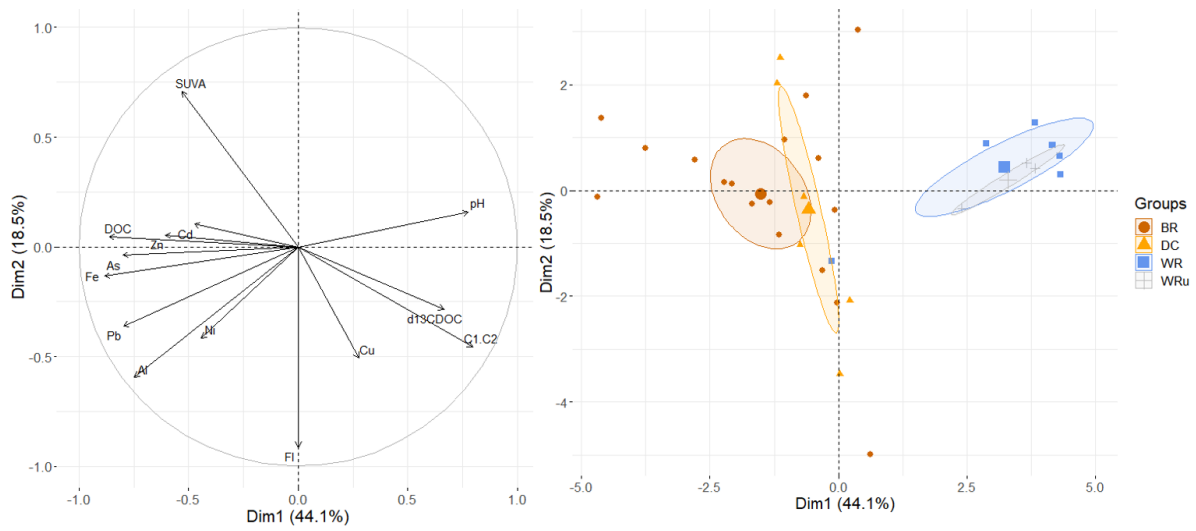
625 **Figure 4:** Ranges of selected TM concentration for different sampled water types. Letters represent significantly
 626 different groups (Kruskall Wallis and Dunn's post hoc multiple test ($p < 0.05$)). The black line is the median. The
 627 lower and upper levels of the box represent the 25 and 75 % quartile, respectively. The lower whisker is smallest
 628 observation greater than or equal to lower hinge - $1.5 * \text{IQR}$ (inter-quartile range). the upper whisker, the upper
 629 whisker is the largest observation less than or equal to upper hinge + $1.5 * \text{IQR}$.

630

631

632

633
634
635
636
637
638

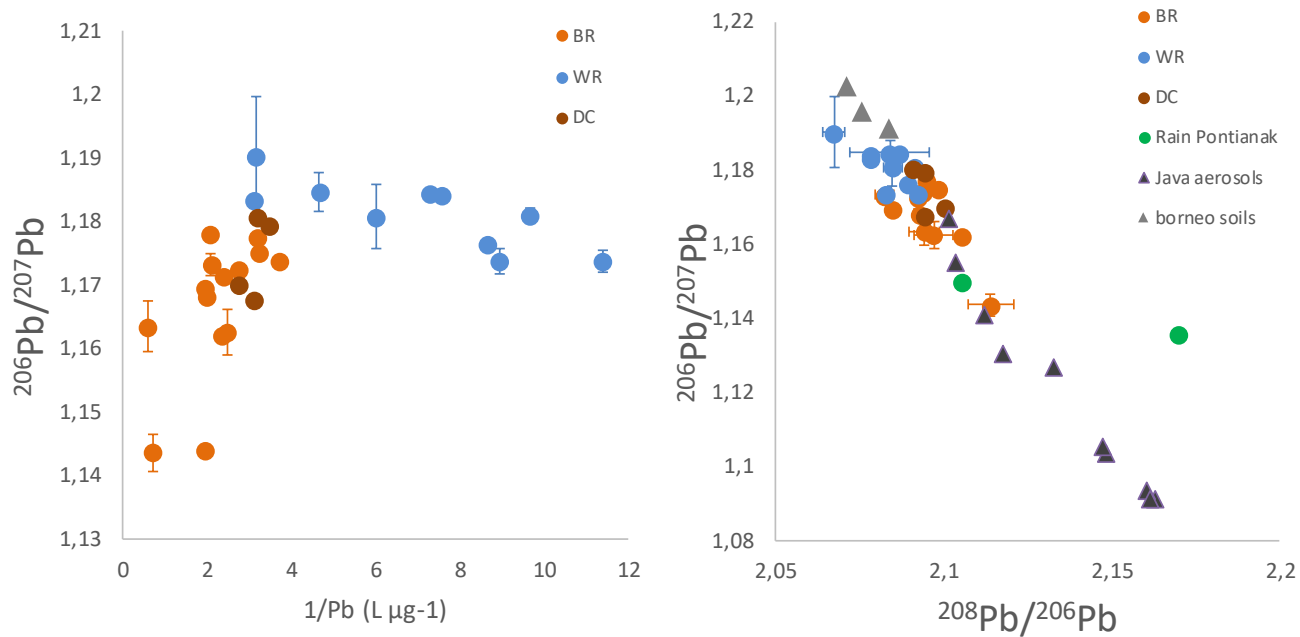


639
640
641
642
643
644
645
646
647
648
649
650
651
652
653
654
655

Figure 5: The first two factors of the PCA (63.1 % of variance) by variables (a) and by observation (b) for the different sampled water types.

656

657



658

659

660 **Figure 6:** (a) Dependence of $^{206}\text{Pb}/^{207}\text{Pb}$ ratio on Pb concentrations for the different water samples. (b) Relationship
661 between $^{206}\text{Pb}/^{207}\text{Pb}$ ratio and $^{208}\text{Pb}/^{206}\text{Pb}$ ratio. The error bars represent the +/- standard deviation.

662

663

664